

Article

Dealing with Negative Inflows in the Long-Term Hydrothermal Scheduling Problem

Paulo Vitor Larroyd ¹, Renata Pedrini ^{2,*} , Felipe Beltrán ¹, Gabriel Teixeira ¹, Erlon Cristian Finardi ^{2,3} 
and Lucas Borges Picarelli ⁴ 

¹ Norus, Florianópolis 88036-003, Brazil; paulo.larroyd@norus.com.br (P.V.L.); felipe.beltran@norus.com.br (F.B.); gabriel.teixeira@norus.com.br (G.T.)

² Department of Electrical and Electronic Engineering, Federal University of Santa Catarina, Florianópolis 88040-900, Brazil; erlon.finardi@ufsc.br

³ INESC P&D Brazil, Santos 11055-300, Brazil

⁴ Norte Energia S.A., Brasilia 70390-025, Brazil; lucaspicarelli@norteenergiasa.com.br

* Correspondence: renata.pedrini@posgrad.ufsc.br; Tel.: +55-(47)996505058

Abstract: The long-term hydrothermal scheduling (LTHS) problem seeks to obtain an operational policy that optimizes water resource management. The most employed strategy to obtain such a policy is stochastic dual dynamic programming (SDDP). The primary source of uncertainty in predominant hydropower systems is the reservoirs inflow, usually a linear time series model (TSM) based on the order- p periodic autoregressive [PAR(p)] model. Although the linear PAR(p) can represent the seasonality and autocorrelation of the inflow datasets, negative inflows may appear during SDDP iterations, leading to water balance infeasibilities in the LTHS problem. Different from other works, the focus of this paper is not avoiding negative inflows but instead dealing with the negative values that cause infeasibilities. Hence, three strategies are discussed: (i) inclusion of a slack variable penalized in the objective function, (ii) negative inflow truncation to zero, and (iii) optimal inflow truncation, among which the latter is a novel approach. The strategies are compared individually and combined. Methodological conditions and evidence of the algorithm convergence are presented. Out-of-sample simulations show that the choice of negative inflow strategy significantly impacts the performance of the resultant operational policy. The combination of strategy (i) and (iii) reduces the expected operation cost by 15%.

Keywords: time series model; river inflow; hydrothermal scheduling; SDDP



Citation: Larroyd, P.V.; Pedrini, R.; Beltrán, F.; Teixeira, G.; Finardi, E.C.; Picarelli, L.B. Dealing with Negative Inflows in the Long-Term Hydrothermal Scheduling Problem. *Energies* **2022**, *15*, 1115. <https://doi.org/10.3390/en15031115>

Academic Editor: Gabriele Di Giacomo

Received: 10 December 2021

Accepted: 27 January 2022

Published: 2 February 2022

Publisher's Note: MDPI stays neutral with regard to jurisdictional claims in published maps and institutional affiliations.



Copyright: © 2022 by the authors. Licensee MDPI, Basel, Switzerland. This article is an open access article distributed under the terms and conditions of the Creative Commons Attribution (CC BY) license (<https://creativecommons.org/licenses/by/4.0/>).

1. Introduction

Given its stochasticity and large scale, it is difficult to find a consistent operational policy for power systems with a predominance of hydroelectric resources. Consequently, the policy is usually obtained in a few steps, wherein the first one consists of solving the long-term hydrothermal scheduling (LTHS) problem. The LTHS focuses on obtaining an optimal policy that minimizes the operational cost over a pluriannual planning horizon, considering constraints related to the operating characteristics of the system and power plants. In such a long horizon, the primary source of uncertainty is associated with the inflows of hydroelectric plants, which are modeled in the LTHS problem by a multistage scenario tree. The breakthrough technique for solving this problem was the development of stochastic dual dynamic programming (SDDP) [1], which breaks the problem down into subproblems that are dynamically solved into two steps: *i*. obtaining trial points (forward pass) and *ii*. building piecewise linear approximations of the cost-to-go functions using the trial points (backward pass). We suggest the reference [2] for an overview of the LTHS problem, describing characteristics related to the formulation of the problem and solution algorithms. Likewise, [3,4] present tutorials regarding the application of SDDP to solve the LTHS problem.

For the inflow's time series modelling (TSM), as widely discussed by [5], some data properties must be captured by generation-scenario models, e.g., time-dependency, seasonality, and spatial correlation. Time-dependency modeling in the SDDP requires special care to guarantee the convergence properties. For instance, work [6] proposes a multi-lag time-dependent structure for a TSM that ensures the cut-sharing requirement of the SDDP method. This multi-lag time-dependent is composed of an independent term, which accounts for the inflow randomness, and a linear combination of the time-dependent terms. This structure is used in the present work to adjust the inflow model to the SDDP algorithm. A similar approach is applied in [7–11], ignoring the independence of the random term.

The SDDP requires a linear TSM (or convex models), which prevents models such as the lag- p periodical autoregressive, in short, PAR(p), from being used on non-normal datasets. As a result, alternative models must be formulated without nonlinear transformations, such as Box–Cox transformation, in the parameter estimation and scenario generation processes. This approach is used in [7–13], wherein a three-parameter log-normal PAR model is estimated for energy and reservoir inflows, respectively. In any case, normalized datasets and multi-lag forecast models that follow the TSM structure of [6] can generate negative inflow values, even if the parameter estimation is computed on a positive dataset. In the LTHS problem, negative inflows can lead to water balance constraint infeasibilities.

Additionally, negative realizations related to other time-dependent TSM, e.g., wind power generation and power demand, in SDDP may cause infeasibilities in the LTHS problem [14]. In this context, this work discusses three strategies, used individually or combined, to deal with this drawback that preserves the statistical properties of the TSM and still guarantees the convergence of the SDDP algorithm. The strategies are:

- **Optimal value:** In this case, an optimal inflow value is obtained by solving a hydraulic resource allocation problem. It is highlighted that this strategy can only be used in the forward pass. As far as we know, this strategy has not yet been explored in literature and consists of finding the optimal value for the inflow that guarantees the hydraulic balance constraint feasibility (even maintaining the inflow negativity).
- **Penalty:** In this strategy, we insert the penalized slack variables in the objective function to assume the exact value, eliminating the nonpositive inflow values.
- **Truncation:** If the inflow is negative, it assumes a value of zero.

Regarding the strategies already presented in the literature, penalty variables are commonly used to handle the negative inflows due to their easy computing implementation, as discussed in [15]. However, it is pointed out that such a strategy generates inconsistencies between the SDDP forward and backward passes, hindering the convergence process. The truncation strategy is based on [12], which indicates the use of a partially truncated model, allowing the generation of negative values by the PAR model. This strategy truncates these values to zero in the SDDP subproblems, preserving the negative value in the cut and the sequence of inflows, i.e., time series statistic properties are maintained. Another similar approach is proposed by [16], in which the truncation point is the minimum historical inflow.

On the other hand, the authors in [17] propose using a first-order multiplicative PAR(p) model compatible with the SDDP algorithm, ensuring positive energy inflow values. Nevertheless, the models' parametrization step must rely on datasets containing only positive values, which may not always be the case for water inflow values. Also, some alternatives to the PAR(p) model are proposed in [18–20].

This work carries out the following procedure to assess the impacts of the optimal value, penalty, and truncated strategies:

1. **Optimization step:** An SDDP run is carried out for each negative inflow strategy. At the end of each SDDP execution is obtained an operational policy.
2. **Simulation step:** The performance of the operational policy (obtained in the optimization step) is assessed via an out-of-sample simulation. The operational cost and the stored energy are considered for the performance comparison.

Thus, the main contributions of this work are:

- Present the main strategies employed in literature to deal with negative inflows (penalty and truncation), as well as propose a novel strategy called optimal value;
- Compare these strategies individually and combine them to improve the operating policy, i.e., an operating policy that performs better in out-of-sample inflow scenarios.

Finally, this paper is organized as follows: Section 2 shows the TSM for river inflow generation and the strategies to deal with negative inflows; Section 3 presents numerical convergence evidence and the assessment of operational policies obtained from different negative inflow strategies. For that, data from the entire Brazilian power system is used. Finally, Section 4 highlights the final remarks.

2. Method

A test power system is used to illustrate the strategies to deal with the negative inflows generated by the TSM. Figure 1 shows the power system’s diagram, composed of two cascaded hydropower plants (HP) and four thermopower plants (TP). These plants meet a constant demand of 450 MW via a single-bus model.

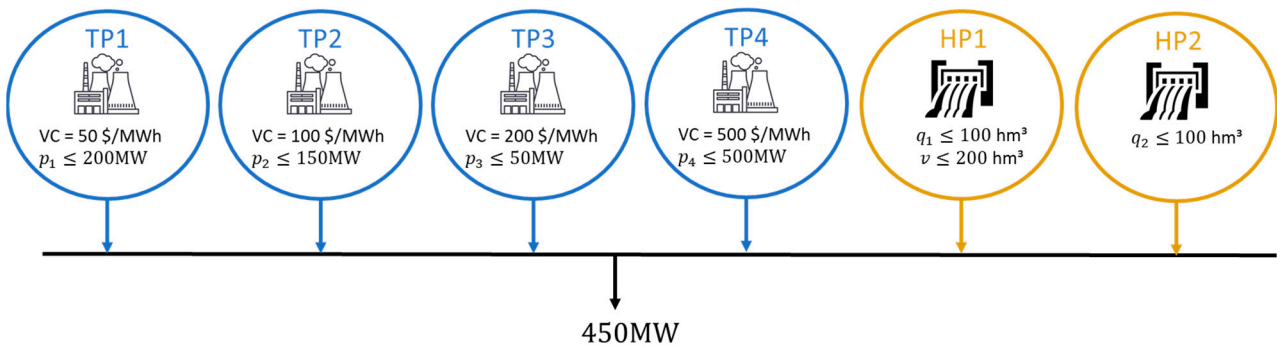


Figure 1. Test system diagram, wherein p_i is the power generation of TP_i , and VC is the associated operating variable cost. Regarding the hydro resources, q_h is the turbined volume of the HP_h , and v is the storage volume of the HP_1 .

The hydraulic coupling of the hydro plants is shown in Figure 2, where the upstream HP_1 can control the amount of water that flows downstream into the run-of-river HP_2 . In this figure, y_h is the incremental inflow volume related to the HP_h .

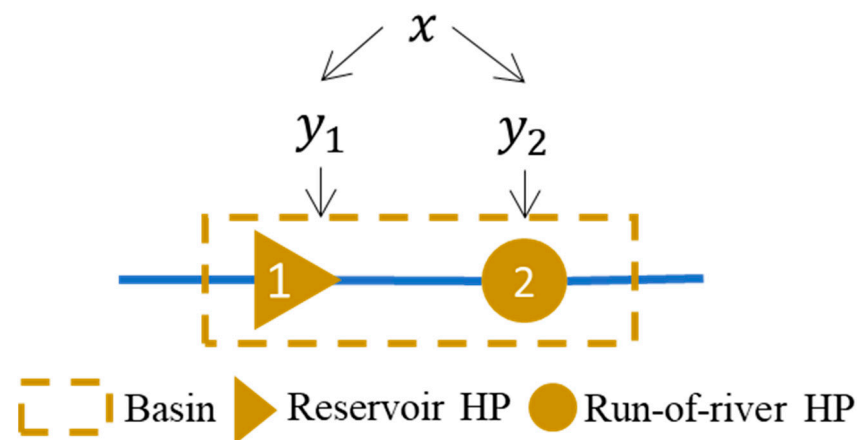


Figure 2. Cascaded hydropower plants.

In this work, we focus on the linear TSM for river inflow with lag p [16,21], described by:

$$x = \sum_{p=1}^P f_p x_{-p} + r, \quad (1)$$

where: x is the generalized inflow forecast; f_p is a linear coefficient; x_{-p} is the past inflow, and r is the model's residual, wherein the randomness is presented.

Using Equation (1), the stochastic process of river inflows may be generalized to river basins, sets of rivers, or reservoirs. The generalized inflow can be decomposed into incremental inflow, for each reservoir h , using the linear transformation:

$$y_h = c_h x + d_h = 0, \quad h = 1, \dots, H. \quad (2)$$

where c_h is the participation coefficient of each hydropower plant in the river basin inflow, and d_h is the degree of freedom of the historical distribution.

Regardless of all the parameters estimation process, the target of this work is how to deal with the negative values of y_h that can lead to an infeasible linear problem (LP) when applying the SDDP algorithm. This test problem is explored for practical reasons, considering one lag of temporal dependence between periods.

Below are described the strategies to deal with the negative inflows.

2.1. Optimal Value Approach

The optimal value is a novel approach that focuses on finding the optimal inflow value that makes the problem feasible. Hence, it is necessary to find the value that does not violate the water balance equation, which can be found by solving a simple hydraulic resource allocation problem. It is important to highlight that the optimal value may still be negative, as long as the LTHS problem becomes feasible. Such behavior aims to find a less relaxed problem, more adherent with the stochastic process. The following subproblem represents one stage of the LTHS problem:

$$zOV(i, x_{-1}) = \min \quad 50p_1 + 100p_2 + 200p_3 + 500p_4, \quad (3)$$

$$\text{s.t. : } p_1 + p_2 + p_3 + p_4 + q_1 + q_2 = 450, \quad (4)$$

$$v + q_1 + s_1 - y_1 = i + l_1^*, \quad (5)$$

$$q_2 + s_2 - y_2 - q_1 - s_1 = l_2^*, \quad (6)$$

$$x = f_1 x_{-1} + r, \quad (7)$$

$$y_h - c_h x = d_h, \quad h = 1, 2, \quad (8)$$

$$0 \leq p_1 \leq 200, \quad 0 \leq p_2 \leq 150, \quad 0 \leq p_3 \leq 50, \quad 0 \leq p_4 \leq 500, \quad (9)$$

$$0 \leq v \leq 200, \quad 0 \leq q_h \leq 100, \quad h = 1, 2 \quad (10)$$

Equation (3) is the operating cost function $zOV(i, x_{-1})$, which is composed of the thermal costs. Constraint (4) is the balance between supply and demand. As can be seen, we assume that hydro generation of HP_h is equal to the q_h . In turn, (5) and (6) are the water balance constraints in the HPs, wherein i is the initial storage volume, and s_h is the spilled volume of HP_h . The terms (l_h^*) are defined as the minimum values that guarantee a feasible subproblem, depending on the values of (i, x_{-1}) . Equation (7) is the inflow related to the river basin considering a lag one dependency into the stochastic process, i.e., the current inflow depends on past time-step inflow. Equation (8) are the incremental inflow volumes from each HP. Equations (9) and (10) are the variable limits.

As the optimal value for inflow volumes (y_h^*) can be previously obtained, the hydraulic resource allocation problem is defined by:

$$w(i, x_{-1}) = \min l_1 + l_2, \quad (11)$$

$$\text{s.t.: } q_1 + s_1 - y_1 - l_1 = i, \quad (12)$$

$$q_2 + s_2 - y_2 - q_1 - s_1 - l_2 = 0, \quad (13)$$

$$x = f_1 x_{-1} + r, \quad (14)$$

$$y_h - c_h x = d_h, \quad h = 1, 2, \quad (15)$$

$$0 \leq l_h \leq \max(-y_h^*, 0), \quad h = 1, 2, \quad (16)$$

$$0 \leq q_h \leq 100, \quad h = 1, 2. \quad (17)$$

The water allocation problem consists of the LTHS equations related to hydroelectric plants and the slack variables for the incremental inflows. Therefore, when the problem (3)–(10) is infeasible, the water allocation problem is solved to define the minimum value of the slack variables (l_h) that makes the problem feasible, and then the LTHS is solved again.

To illustrate this approach, the cost function, $zOV(i, x_{-1})$, is assessed for a range of initial volumes with the past inflows, considering $r = 1$, $f_1 = 0.5$, $c_1 = 0.25$, $c_2 = 0.75$, $d_1 = 10$, $d_2 = 5$. The result is shown in Figure 3. It is clear that $zOV(i, x_{-1})$ is non-convex, which makes impossible the use of the optimal value approach in the SDDP backward phase. Using a 2D approximation for the function on $i = 0$, Figure 4 shows the optimality cuts (orange lines), approximating the cost function (blue line). Note that when the function is non-convex, the cut (orange dashed line) fails to be a valid lower bound for the cost function. Another approach can be implemented to solve this issue, as described in the following sections.

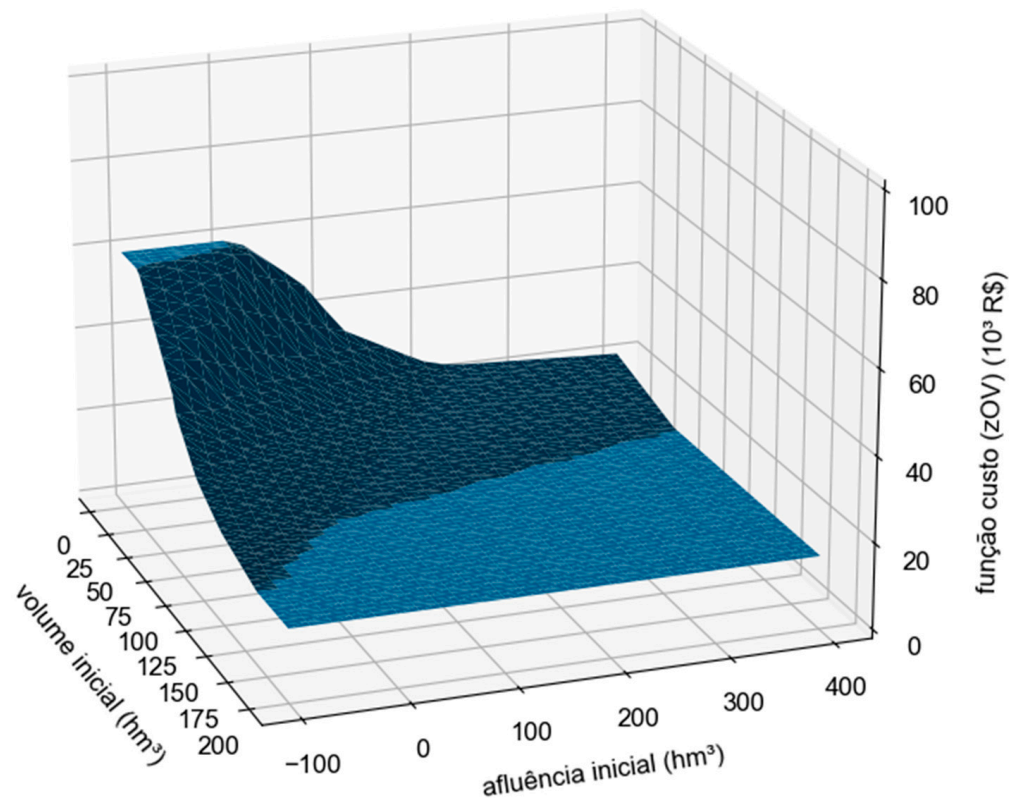


Figure 3. Cost function (zOV) (10^3 \$) per initial volume (hm^3) and initial inflow (hm^3).

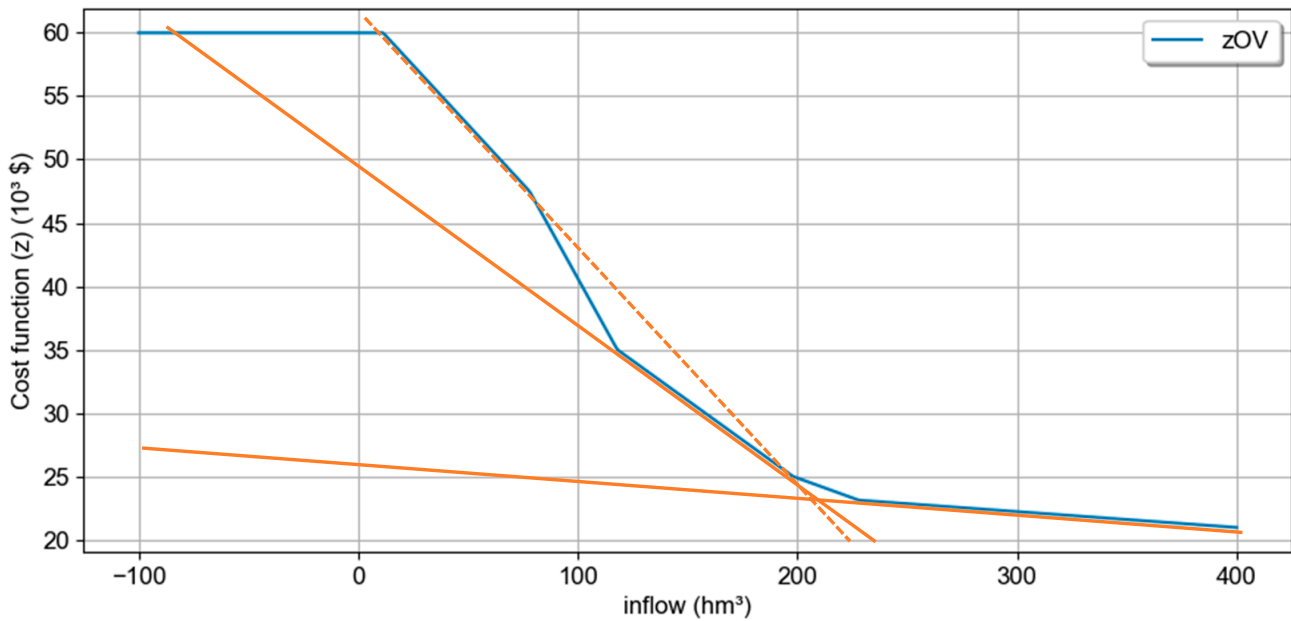


Figure 4. Cost function (zOV) (10^3 \$) per inflow (hm^3) with the optimality cuts (orange) approximating the cost function.

2.2. Penalty

In the penalty approach, a slack variable is included to assume the exact value to eliminate the inflow's negativity, and it is penalized in the objective function. Therefore, $z(i, x_{-1})$ receives a new element that penalizes (l_h):

$$zP(i, x_{-1}) = \min 50p_1 + 100p_2 + 200p_3 + 500p_4 + k_1l_1 + k_2l_2, \quad (18)$$

$$\text{s.t. : } p_1 + p_2 + p_3 + p_4 + q_1 + q_2 = 450, \quad (19)$$

$$v + q_1 + s_1 - y_1 - l_1 = i, \quad (20)$$

$$q_2 + s_2 - y_2 - q_1 - s_1 - l_2 = 0, \quad (21)$$

$$x = f_1x_{-1} + r, \quad (22)$$

$$y_h - c_hx = d_h, h = 1, 2, \quad (23)$$

$$0 \leq p_1 \leq 200, 0 \leq p_2 \leq 150, 0 \leq p_3 \leq 50, 0 \leq p_4 \leq 500, \quad (24)$$

$$0 \leq v \leq 200, 0 \leq q_h \leq 100, h = 1, 2, \quad (25)$$

$$l_h \geq 0, h = 1, 2. \quad (26)$$

A critical point in this strategy is the definition of the penalty value (k_h). If this value is too low, the model may use the slack variable such as a "thermal power plant," generating energy based on a cost per MW payment. Defining the penalty with the same value as the most expensive thermal (500\$), we have the result of Figure 5a. For a multistage problem, this strategy is even more critical because there is no guarantee the penalty value does not allow an excess of virtual water l_h or, even worse, overprices the cost to go function, once critical scenarios are evaluated in the SDDP framework.

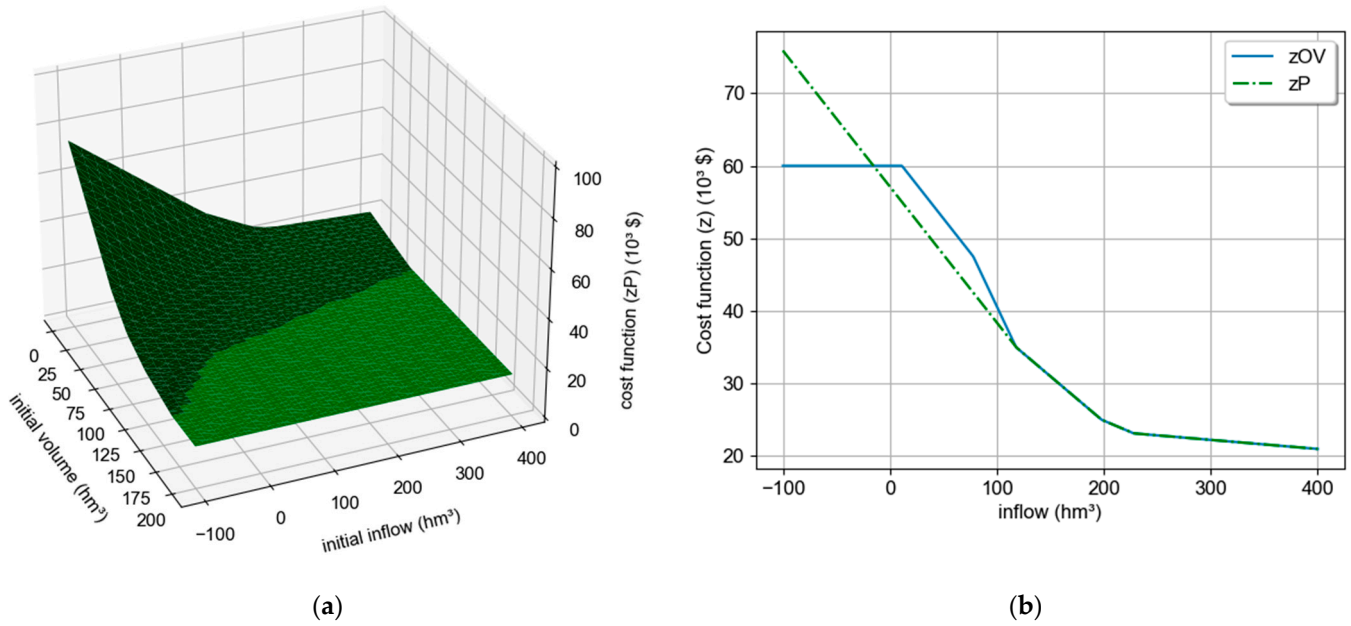


Figure 5. (a) Cost function (zP) (10³ \$) per inflow (hm³) by the penalty approach. (b) penalty approach (dashdot green), and optimal value approach (blue).

Note that the use of the penalty approach also convexifies the function, for which Figure 5b shows the comparison between the penalty and the optimal value approach, considering $i = 0$. As the slack variable value is defined by optimization, the penalty strategy provides a good approximation of the cost function. However, when the slack variable is used, the slope of the function is defined by the penalty value.

2.3. Truncation

Another way to deal with the infeasibilities produced by the negative inflows is the truncation approach proposed in [12]. By this approach, there is a condition that, if ($y_h \leq 0$), the slack variable (l_h) assumes the inverse of the negative inflow, as follows:

$$zT'(i, x_{-1}) = \min 50p_1 + 100p_2 + 200p_3 + 500p_4 \tag{27}$$

$$\text{s.t. : } p_1 + p_2 + p_3 + p_4 + q_1 + q_2 = 450, \tag{28}$$

$$v + q_1 + s_1 - y_1 - l_1 = i, \tag{29}$$

$$q_2 + s_2 - y_2 - q_1 - s_1 - l_2 = 0, \tag{30}$$

$$x = f_1x_{-1} + r, \tag{31}$$

$$y_h - c_hx = d_h, h = 1, 2, \tag{32}$$

$$l_h = \max(-y_h^*, 0), h = 1, 2, \tag{33}$$

$$0 \leq p_1 \leq 200, 0 \leq p_2 \leq 150, 0 \leq p_3 \leq 50, 0 \leq p_4 \leq 500, \tag{34}$$

$$0 \leq v \leq 200, 0 \leq q_h \leq 100, h = 1, 2. \tag{35}$$

Figure 6a shows the cost function using the truncation approach.

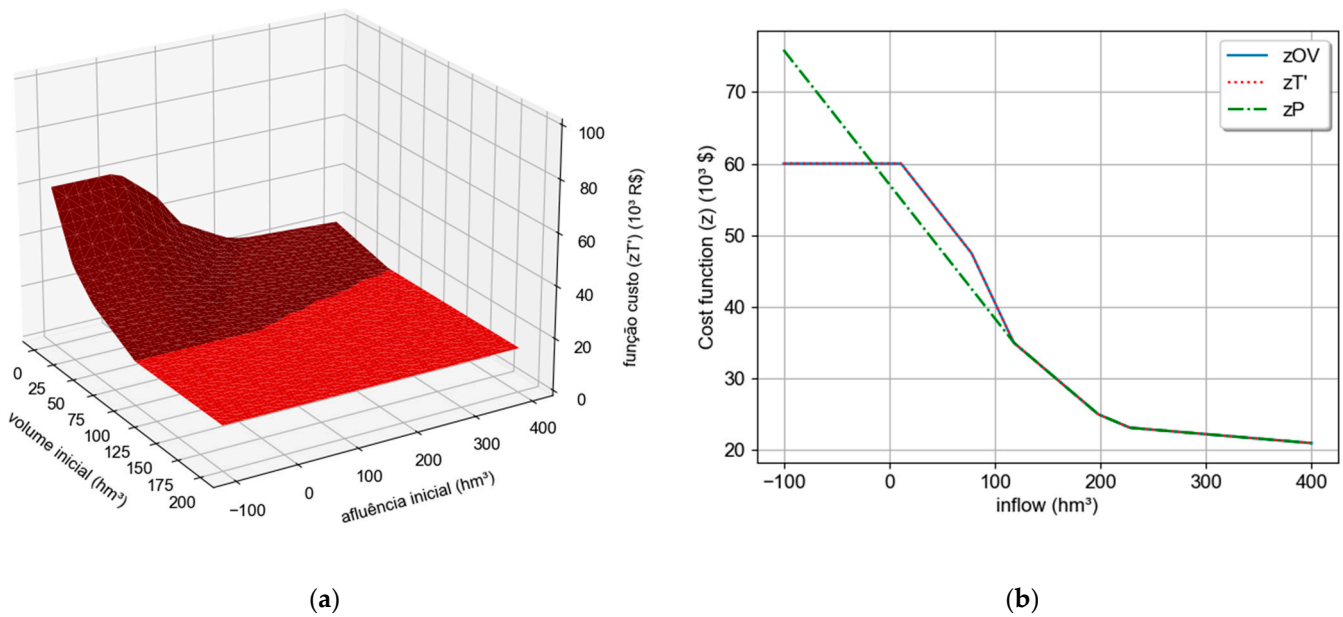


Figure 6. (a) Cost function (zT') (10^3 \$) per inflow(hm^3) by the truncation approach. (b) Comparison between the cost function (z) (10^3 \$) by the optimal value approach (solid blue), truncation approach (dotted red), and penalty approach (dash and dot green).

It is clear that the approach proposed in [12] produces a non-convex function for a substantial part of $zT'(i, x_{-1})$ domains, since the TSM used in the previous problem is a generalized model for the river basin, following the scheme of Figure 2. To produce a convexified problem, at least for most of the $zT'(i, x_{-1})$ domain, the slack variable must be added to compensate (x) as following:

$$zT(i, x_{-1}) = \min 50p_1 + 100p_2 + 200p_3 + 500p_4 \quad (36)$$

$$\text{s.t. : } p_1 + p_2 + p_3 + p_4 + q_1 + q_2 = 450, \quad (37)$$

$$v + q_1 + s_1 - y_1 = i, \quad (38)$$

$$q_2 + s_2 - y_2 - q_1 - s_1 = 0, \quad (39)$$

$$x = f \cdot x_{-1} + r, \quad (40)$$

$$y_h - c_h \cdot (x + l) = d_h, \quad h = 1, 2, \quad (41)$$

$$0 \leq p_1 \leq 200, 0 \leq p_2 \leq 150, 0 \leq p_3 \leq 50, 0 \leq p_4 \leq 500, \quad (42)$$

$$0 \leq v \leq 200, 0 \leq q_h \leq 100, h = 1, 2 \quad (43)$$

$$l = \max(\max(-d_1/c_1, -d_2/c_2) - x^*, 0) \quad (44)$$

The corrected $zT(i, x_{-1})$ of the truncation approach is shown in Figure 7.

Besides the constant behavior at the beginning of $zT(i, x_{-1})$, wherein $-100 \leq x_{-1} \leq 78$, the rest of the function is convex, and the cuts are valid inferior boundaries. Therefore, the truncation approach implies that $zT(i, x_{-1})$ will be convexified by the cuts in the SDDP framework. However, this also implies that the estimation of the cost function's lower and upper bounds must be reviewed for the SDDP framework, as discussed in Section 2.1.

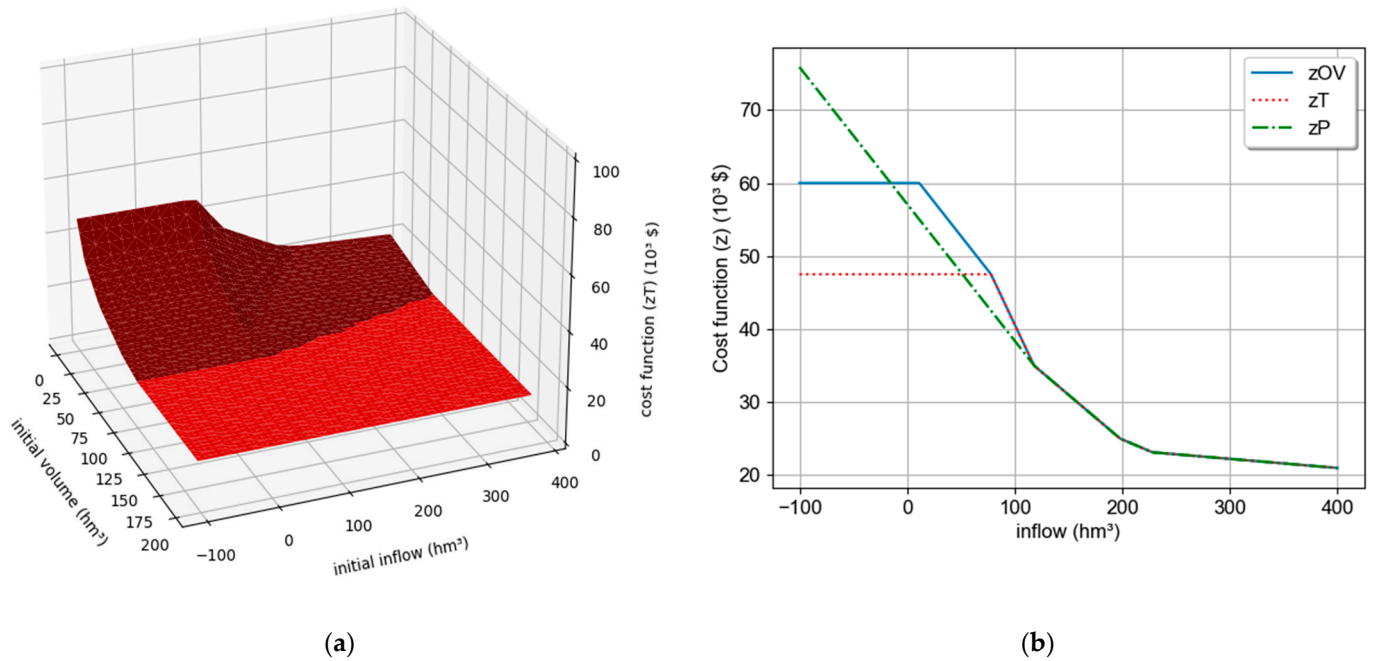


Figure 7. (a) Cost function (zT) (10^3 \$) per inflow (hm^3) by the truncation approach. (b) Comparison between the cost function (z) (10^3 \$) by the optimal value approach (solid blue), truncation approach (dotted red), and penalty approach (dash and dot green).

A key point for the use of the generalized truncation approach is the difference between the ratios (d_h/c_h) of the reservoirs of the same river basin. According to Equation (44), the higher is the difference, the more relaxed is the version of $zT(i, x_{-1})$ obtained. In this case, a better approach is to formulate a TSM for each reservoir, where ($c_h = 1$).

2.4. Truncation Combined with Penalty

A better version of the formulation of $zT(i, x_{-1})$, i.e., as close to $z(i, x_{-1})$ as possible, can be defined by combining truncation and the penalty formulations. The slack variable is now both truncated and penalized as follows:

$$zTP(i, x_{-1}) = \min 50p_1 + 100p_2 + 200p_3 + 500p_4 + kl, \quad (45)$$

$$\text{s.t. : } p_1 + p_2 + p_3 + p_4 + q_1 + q_2 = 450, \quad (46)$$

$$v + q_1 + s_1 - y_1 = i, \quad (47)$$

$$q_2 + s_2 - y_2 - q_1 - s_1 = 0, \quad (48)$$

$$x = f \cdot x_{-1} + r, \quad (49)$$

$$y_h - c_h \cdot (x + l) = d_h, \quad h = 1, 2, \quad (50)$$

$$0 \leq p_1 \leq 200, 0 \leq p_2 \leq 150, 0 \leq p_3 \leq 50, 0 \leq p_4 \leq 500, \quad (51)$$

$$0 \leq v \leq 200, 0 \leq q_h \leq 100, \quad h = 1, 2, \quad (52)$$

$$0 \leq l \leq \max(\max(-d_1/c_1, -d_2/c_2) - x^*, 0). \quad (53)$$

Therefore, the slack variable is bounded by zero and the maximum value between the individual power plant incremental inflows. The resultant cost function $zTP(i, x_{-1})$ is presented in Figure 8.

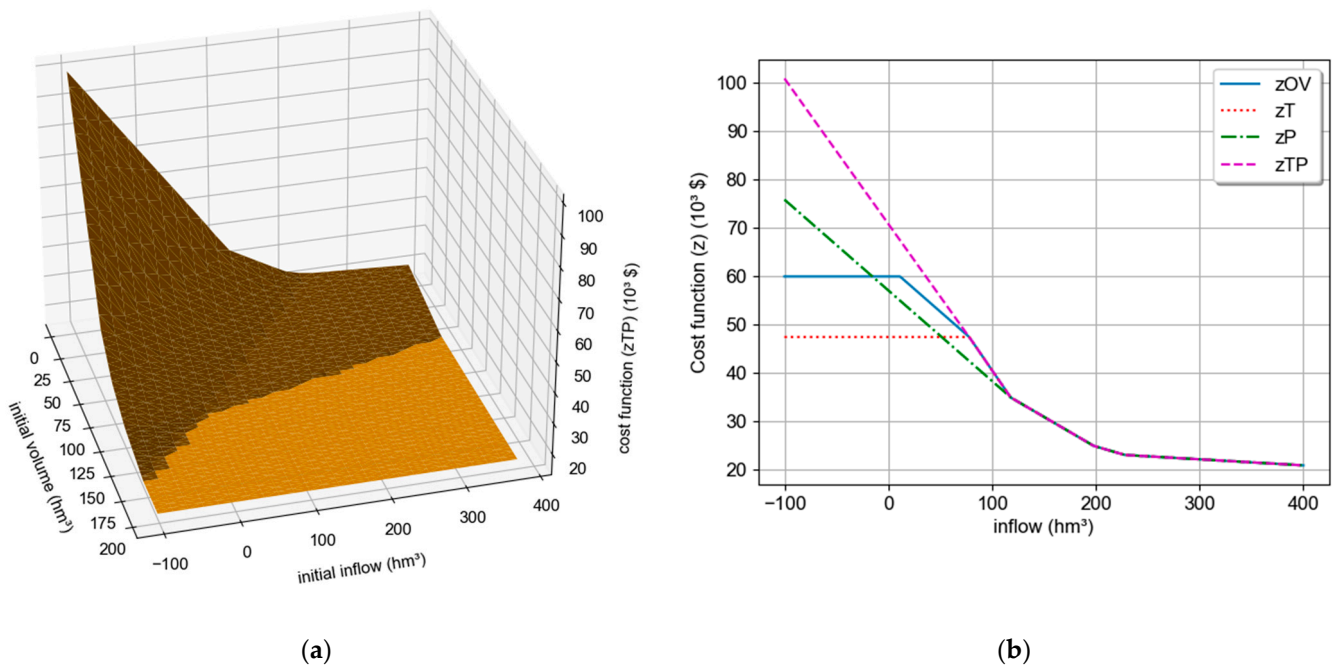


Figure 8. (a) Cost function (zTP) (10^3 \$) per inflow(hm³) by the truncation approach. (b) Comparison between the cost function (z) (10^3 \$) by the optimal value approach (solid blue), truncation approach (dotted red), penalty approach (dash and dot green), and penalty with truncation (dashed magenta).

2.5. Convergence Criteria

As mentioned in the previous sections, the non-convex parts of $zT(i, x_{-1})$ and $zTP(i, x_{-1})$ will be convexified by the cuts computed in the SDDP framework. Therefore, depending on the values of (i, x_{-1}) , the results of the primal LP problems of $zT(i, x_{-1})$ and $zTP(i, x_{-1})$ formulated in the previous sections will be lower than the convexified version of these functions on their master problems, i.e., LP problems composed of the cuts. To illustrate this behavior, the primal and master problems of $zT(i, x_{-1})$ are shown in Figure 9 for $(i = 0)$ and a range of values of (x_{-1}) :

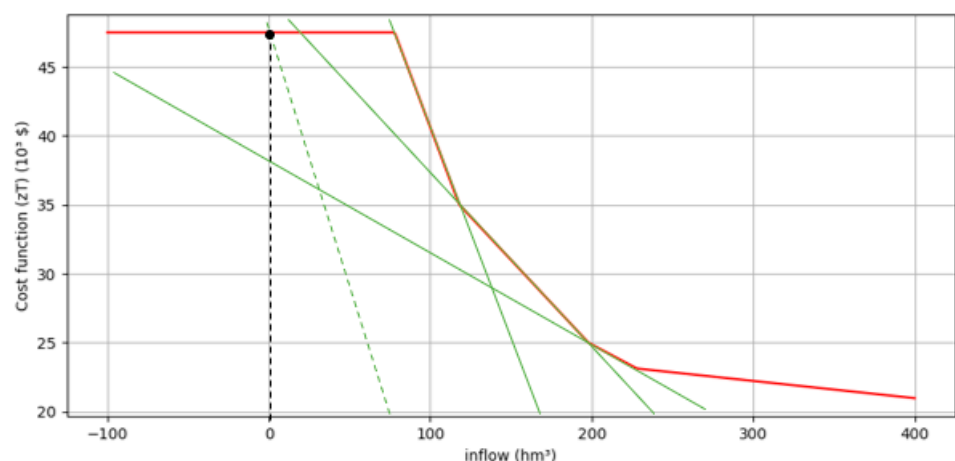


Figure 9. Primal LP problem of $zT(i, x_{-1})$ (red line) and cuts formulated to convexify the problem (green lines).

For $(x_{-1} < 80)$, the value of the primal problem (blue line) is lower than the value of the cut activated on the master problem, which means that the value of the primal problem may not be a good estimator for the upper bound of the operational cost function, especially in the non-convex domain.

Therefore, the lower and upper bounds must be estimated by the solution of the current master problem. In the SDDP framework, this means that a new version of the master problem must be solved at the forward pass exclusively to estimate the lower and upper bounds. Since the SDDP combines the primal problem of a stage (t) with the master problem of the next stage ($t + 1$), the new master problem must be formulated for each stage t depending on the inputs of scenario s as presented in (54)–(57):

$$z_{TP,t}^{M,s}(i_t^s, x_{t-1}^s) = \min z_t, \tag{54}$$

$$\text{s.t. : } z_t - \sum_{r=1}^{R_t} \rho_{r,t} z_{r,t} = 0, \tag{55}$$

$$z_{r,t} \geq b_{r,t}^j - \pi_{r,t}^j i_t^s - \delta_{r,t}^j x_{t-1}^s, \quad r = 1, \dots, R_t, j = 1, \dots, J, \tag{56}$$

$$z_t \geq 0, \quad z_{r,t} \geq 0, \quad r = 1, \dots, R_t. \tag{57}$$

where (R_t) is the number of realizations in t ; ($z_{r,t}$) and ($\rho_{r,t}$) are respectively the cost and the probability of the realization (r) in (t); (z_t) is the expected cost in (t), and ($b_{r,t}^j$), ($\pi_{r,t}^j$), ($\delta_{r,t}^j$) are respectively the operational cost and the cut's RHS and slope coefficients.

Assuming a multistage problem with (T) stages and (S) scenarios, the lower and upper bounds must be computed as shown in (58) and (59), respectively.

$$z_{LB} = z_{TP,1}^M, \tag{58}$$

$$z_{UB} = \sum_{s=1}^S \left(\prod_{t=1}^T \rho_{m(s,t),t} \right) \cdot \left(z_{TP,1}^M + \sum_{t=2}^T z_{m(s,t),t}^* - z_{TP,t}^{M,s} \right). \tag{59}$$

where: (m) maps the realization (r) associated with scenario (s) and stage (t).

3. Results

This section compares the proposed strategies to deal with negative inflow values using the Brazilian long-term hydrothermal scheduling problem. The Brazilian interconnected power system comprises 163 hydropower plants (97 are run-of-river) and 127 thermal power plants. The goal of the problem is to satisfy the demand at the lowest possible cost with a risk-averse measure, considering five years divided into monthly time-steps. Figure 10 shows the power availability and demand.

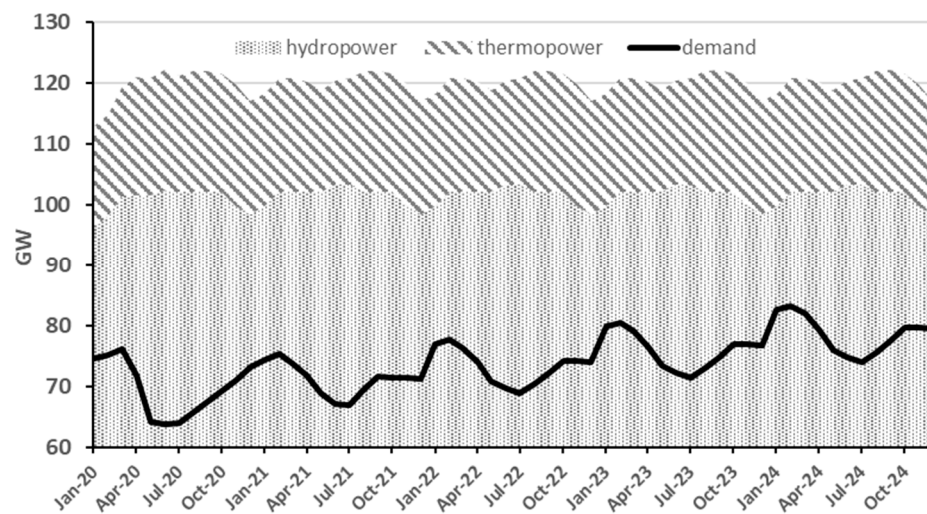


Figure 10. Power availability and demand.

The inflows are modeled into a multistage scenario tree using a PAR model with maximum order 6. This work considers a TSM for the 21 river basins of the system. Figure 11 shows a comparison of the natural energy between the historical data scenarios (repeating

its values for all years as a benchmark), the observed inflow scenario from January 2020 to October 2021, and the inflow scenarios randomly obtained for the optimization process (8160 scenarios) and the simulation step (2000 scenarios), both presented in Section 3.2. Note that the realizations for the first three months obtained by the TSM model present scenarios below the average of the historical natural energy, which is due to the inflow trend in the PAR model before January 2020. The rest of the TSM scenarios are entirely aligned with the historical data. It is highlighted that the observed inflow scenario from January 2020 is an outlier (severe scenario) of the historical dataset.

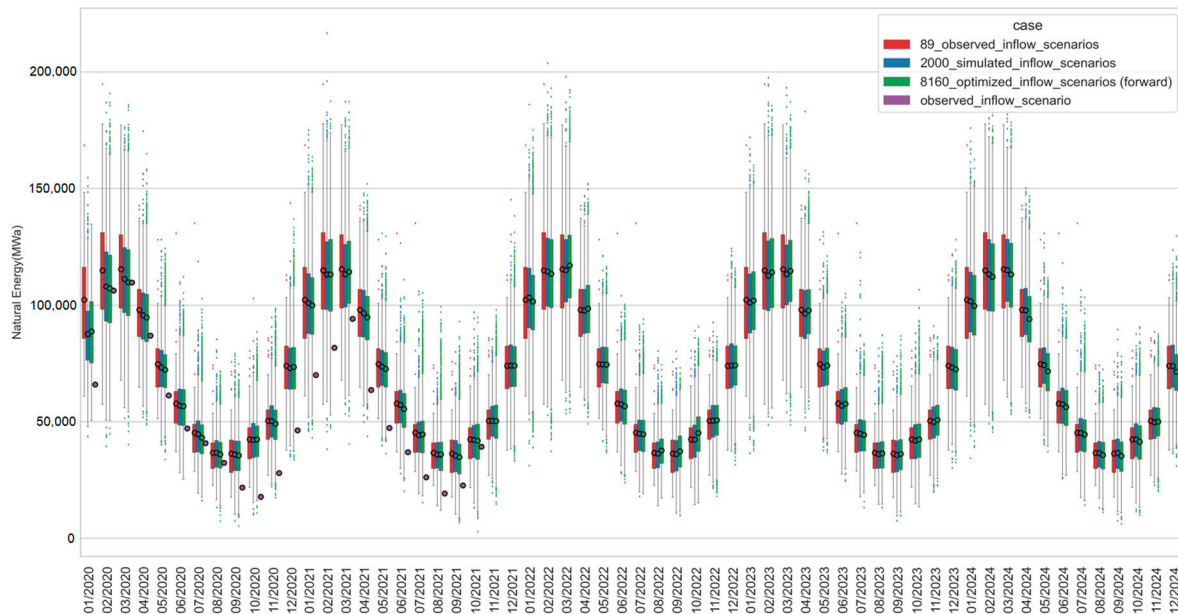


Figure 11. This figure shows the historical inflow realizations (red), the 2000 inflow series used in the simulation step (blue), the 8160 scenarios used at the optimization (green), and the observed inflow scenario from January 2020 to October 2021.

The results are divided as follows: Section 3.1 presents an algorithm's convergence proof for the different strategies to deal with negative inflow values. In addition, Section 3.2 indicates the SDDP considerations to obtain the operational policy assessed in an out-of-sample simulation and considering the observed inflow scenario.

3.1. Whole Tree Optimization

Initially, the optimization is performed by solving the whole tree to prove the validity of the algorithm's convergence, as pointed out in Section 2.5. As the problem grows exponentially with the number of stages, a reduced problem is considered to solve the whole tree, with two inflow residual realizations per stage and an optimization horizon of 10 stages.

Figure 12 shows the convergence of the SDDP algorithm considering the truncation, penalty, and truncation combined with penalty strategies. The figure shows that the gap between the lower and upper bound for each strategy is below 0.1%. In this way, the figure proves that, when adopting the truncation strategy, or truncation associated with the penalty, it is necessary to change the calculation of the lower and upper bounds, according to Section 2.5, so that the algorithm converges.

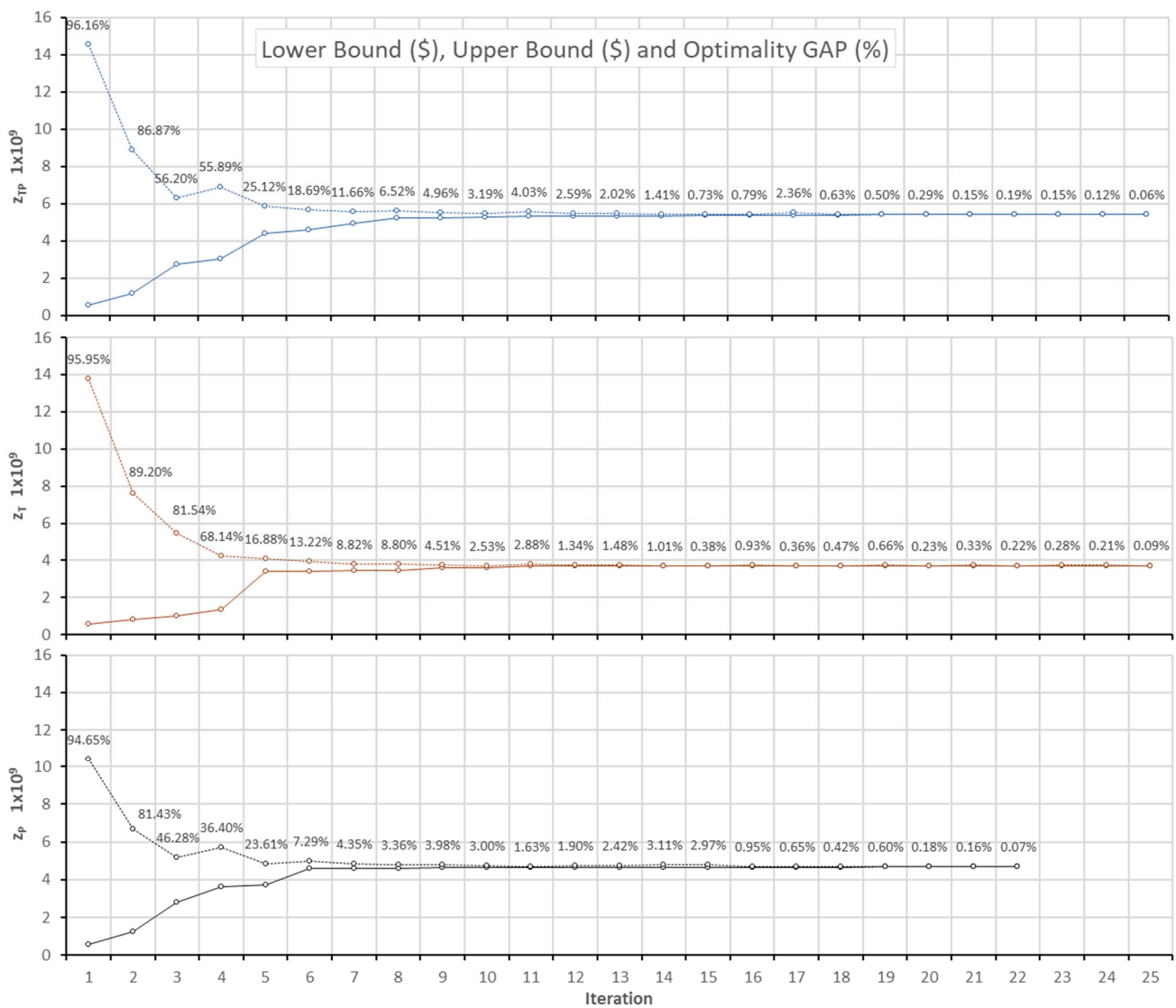


Figure 12. System capacity and demand.

Moreover, the strategies do not converge to the same value since each strategy deals differently with negative inflow. For instance, the truncation strategy converges to the lowest value, which does not indicate this is the best strategy. As the truncation strategy sets the negative inflows equal to zero, this strategy most relaxes the problem. The following section compares the strategies to a large scenario tree with a subsequent simulation of the operation policy obtained in the optimization step.

3.2. Stochastic Optimization and Operational Policy Simulation

This work considers the following SDDP settings for the optimization process:

- 85 iterations (forward/backward steps);
- 96 forwards per iteration distributed in a synchronous parallel setting. At the end of the whole optimization, 8160 scenarios are optimized;
- 96 inflow realizations per stage;
- Five years horizon with monthly stages;
- Selection cut strategy of [22];
- CVaR_{1- α} with parameters $\alpha = 0.25$ and $\lambda = 0.5$.

Below are the cases compared in this study:

- Trunc.: Forward and backward steps use the truncation strategy of Section 2.3;

- O.V + Trunc.: Forward uses the optimal value approach, and the backward step uses the truncation approach;
- Trunc. & Pen.: Forward and backward steps use the truncation combined with the penalty strategy as presented in Section 2.4;
- O.V + Trunc. & Pen.: Forward step uses the optimal value approach, and backward step uses truncation with penalty;
- Pen.: Forward and backward steps use the penalty approach of Section 2.2;
- O.V + Pen: The forward step uses the optimal value approach, and the backward step uses the penalty approach.

Figure 13 compares the lower-bound evolution throughout 85 iterations of the optimization process. The iteratively random selection of different first-stage realizations is responsible for the lower-bound drops between iterations. Note that the negative inflow strategy has a considerable impact on the lower bound of the problem. For instance, the lower bound level of case O.V Trunc & Pen increases 1.5 times compared to the O.V Pen. However, as the penalty strategy consists of penalizing the slack variable related to the negative inflow, the lower bound of the strategies that involve penalty are, in any case, superior to the others. Therefore, the lower bound is not comparable between all strategies.

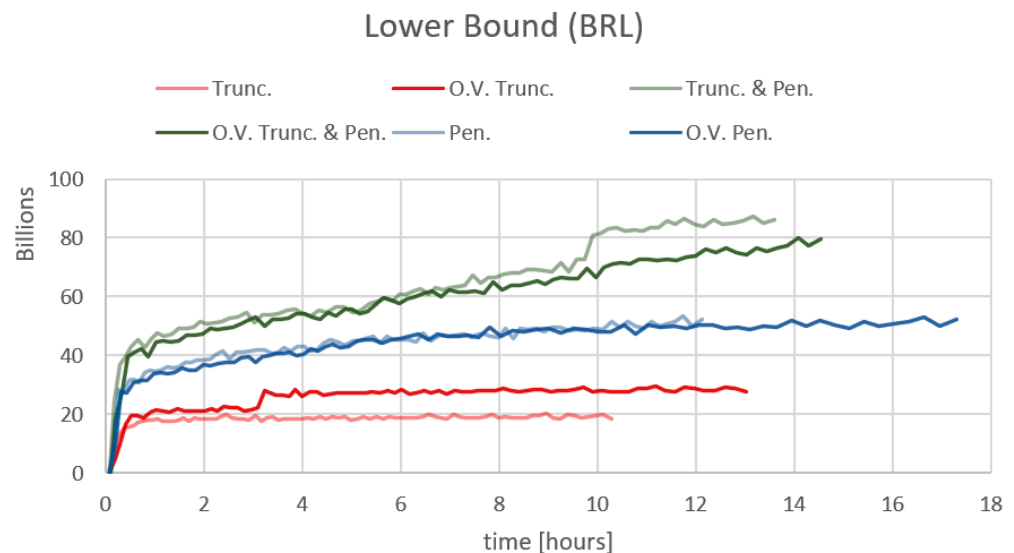


Figure 13. Optimization process—Lower bound evolution per time.

At the end of the optimization process, a set of approximations (cuts) of the cost-to-go functions are obtained per stage. These cuts are an operational policy since they have the information (future water cost) of how the hydro resources must be used. The following sections assess the operational policy obtained for all cases with two simulations: *i.* 2000 out-of-sample scenarios and *ii.* the observed inflow scenario between 2020 and 2021. The simulation process uses the same hydrothermal system configuration as the optimization process.

3.2.1. Out-of-Sample Simulation

The out-of-sample simulation aims to verify the performance of the policy (optimality cuts) obtained in the optimization step in scenarios different from those used in the optimization. For this simulation, 2000 scenarios are used, which has the distribution shown in Figure 11.

Figure 14 presents the operational costs obtained simulating the policy obtained from all cases tested. As it can be noticed, the higher operational cost is obtained using the truncation strategy. When Figures 13 and 14 are compared, the truncation strategy has the lowest optimization cost in Figure 13 and the highest simulation cost in Figure 14. This

fact suggests that the truncation strategy relaxes the problem. Therefore, as the problem does not have to deal with the most critical scenarios in optimization, its policy is less risk-averse.

Out-of-Sample Simulation - Operational Costs (BRL)

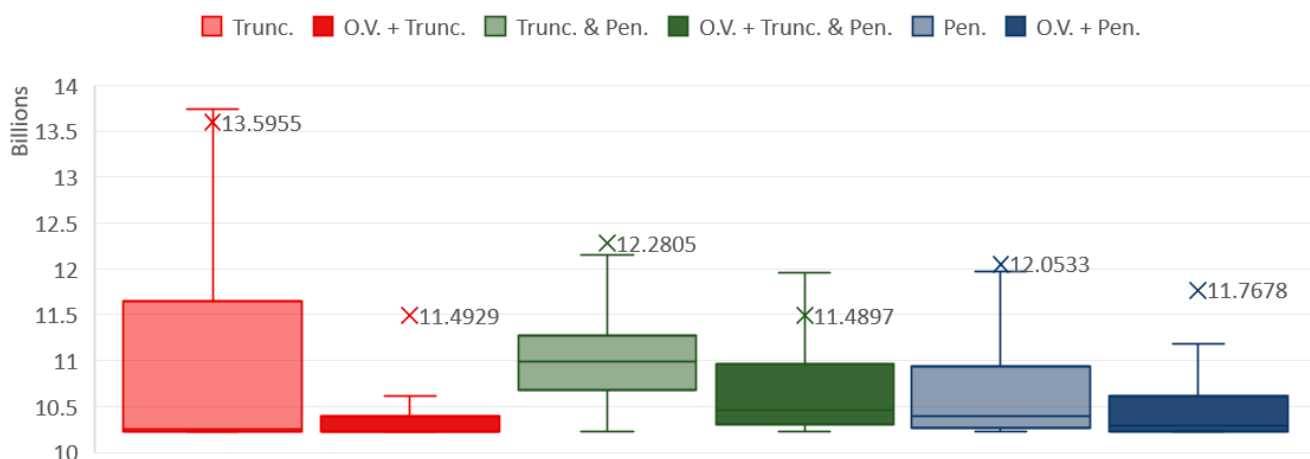


Figure 14. Operational costs (BRL) from the out-of-sample simulation. The X's represent the average operational cost.

On the contrary, the strategy with the lowest average operational cost is the O.V + Trunc. & Pen, which combines the three strategies proposed. This strategy seeks to be more austere in the backward step when the optimal value strategy cannot be used. Thus, it only allows the slack variable to assume values greater than zero when there is a negative inflow value and makes its value the closest to necessary, avoiding the penalty. A similar average cost is obtained by combining the truncation strategy with the optimal value. However, it is essential to point out that the policy obtained with the O.V + Trunc. result in an asymmetrical distribution of costs since the mean value of the distribution is displaced from the boxplot, showing the existence of outliers with very high costs. Therefore, in wet scenarios, the strategy behaves well; however, when some extreme scenario presents itself, the system does not reserve enough water and needs to dispatch more expensive thermopower plants and increase the deficit risk.

Comparing the Truncation operational cost with the one from O.V + Trunc. and O.V + Trunc. & Pen, the former has an average cost 15% higher than the latter.

Furthermore, it is significant to note that the penalty strategy, widely used in the literature, presents an average operational cost 11% lower than the truncation strategy, being the best strategy among the two. However, the penalty also results in a 5% higher cost than the O.V + Trunc strategy or O.V. + Trunc. & Pen. and 2% higher than O.V. + Pen, which shows that the optimal value strategy, first presented in this study, makes the calculated policy more consistent with reality.

Figure 15 exhibits the stored energy for all cases in the percentage of the maximum energy stored in the reservoirs. The energy stored level in the reservoir can impact how much energy needs to be dispatched from the thermopower plants at each stage. When the system stores less water in the reservoirs, it is believed that this energy supply is not needed; on the other hand, if some extreme scenario materializes, there may not be enough water to supply demand, and costly thermal power plants have to be dispatched. Thus, Figure 15 shows that the truncation strategy results in more empty reservoirs, revealing that this strategy does not prepare the system for the risk of future droughts.

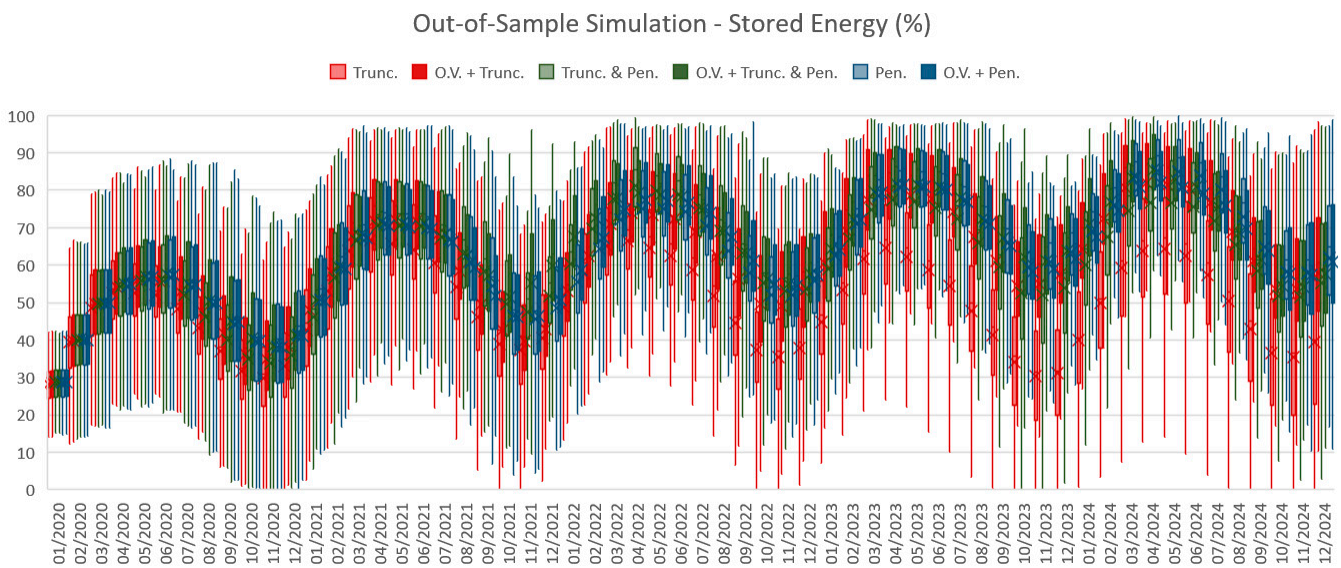


Figure 15. Stored energy obtained by out-of-sample simulation in the percentage of the maximum stored energy of the system.

Moreover, strategies without truncation save more water in the reservoirs as they do not have the same level of relaxation in the problem.

3.2.2. Observed Inflow Scenario

This subsection tests the policy in the observed inflow scenario, referring to January 2020 to October 2021. As shown in Figure 11, the performed scenario is an outlier and critical from a hydrological point of view.

Figure 16 shows the marginal cost found for the southeast subsystem of the Brazilian power system. This subsystem is the most important in Brazil, with the most significant demand to be met and the most remarkable power generation capacity.

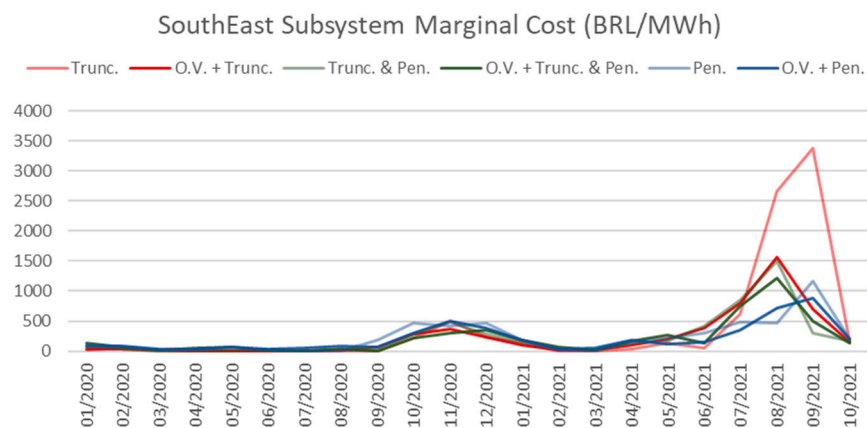


Figure 16. Marginal cost (BRL/MWh) related to the southeast subsystem.

Note that the truncation strategy presents a peak in its marginal costs in August and September 2021, which shows that it did not take precautions against a critical inflow scenario, resulting in the need to dispatch more expensive thermopower plants. On the contrary, the scenarios with lower marginal cost peaks involve the optimal value strategy. For all combinations (Trunc., Trunc. & Pen. And Pen.), when the optimal value strategy is added, the marginal cost decreases, showing that the use of this strategy tends not to relax the problem as much, since the inflow is only modified enough to avoid the problem infeasibility.

This behavior is also observed in Figure 17, which shows the storage level in the reservoirs for each tested strategy. The results for the cases involving the truncation strategy are the ones that present smaller storage values, while the ones that involve the penalty strategy are the ones that result in larger storage values.

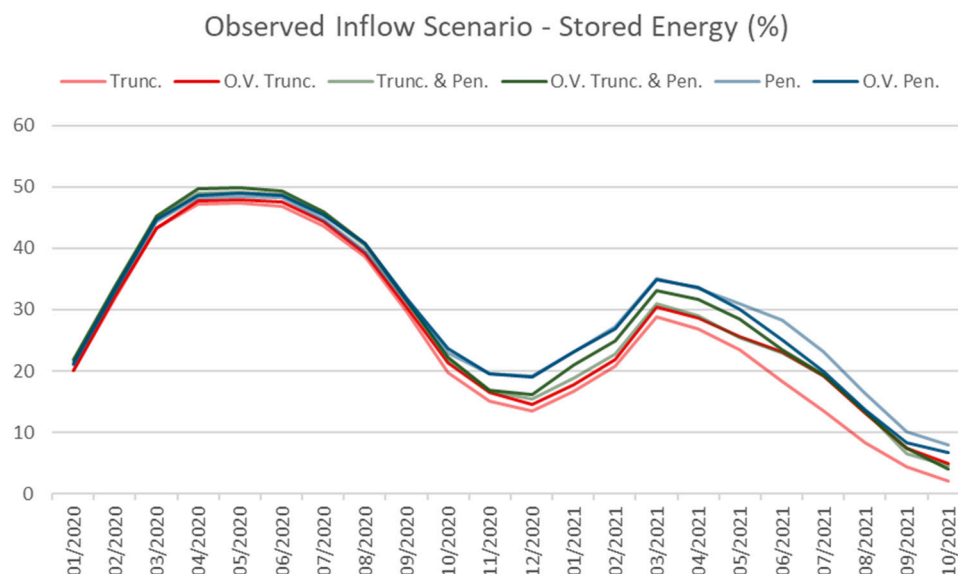


Figure 17. Stored energy obtained by the observed scenario in the maximum system's stored energy percentage.

While interesting, it is essential to note that the observed scenario is critical, so the policy must operate a system in an extreme situation.

4. Conclusions

To sum up, this study has presented a comparison between strategies to deal with negative inflows in the LTHS problem. First, it was discussed how negative inflows occur in the problem, which may arise from the TSM model or negative values presented in the historical observations. Then, three strategies are presented to deal with the infeasibilities caused by negative inflows and the combination of these strategies.

The main conclusion of this study is that, despite being a problem seldom discussed in the literature, the strategy to deal with negative inflows dramatically affects the operation policy obtained in the optimization of the LTHS problem.

When considering the truncation strategy, which is the most relaxed strategy to deal with negative inflows, the operational cost can be 15% higher than the O.V + Truncation and O.V + Truncation & Pen strategies present the lowest operational cost. This result also shows that the optimal value strategy, first presented in this work, results in operational policy that better represents the uncertainties since, through this strategy, the least possible relaxation of the problem is sought. Despite providing a better solution, it is important to emphasize that the optimal value strategy increases the complexity of the implementation and solution of the problem, since, if the negative inflow causes infeasibility, in addition to solving each stage a LTHS subproblem, it is also necessary to solve a problem of hydraulic resources allocation.

Furthermore, when the policy was tested in a real and critical scenario, the marginal cost obtained by applying the truncation strategies showed sharp peaks, which demonstrates that the relaxation makes it unable to protect itself against more extreme scenarios, since it does not feel the need to store enough water.

For future work, it is important to compare the strategies in a model that considers the inflows of hydropower plants individually and does not aggregate them by river

basins. In an individualized system, inflow negativity is more present and can change the strategies performance.

Author Contributions: Conceptualization, P.V.L.; Data curation, P.V.L., R.P., F.B. and G.T.; Formal analysis, P.V.L., R.P. and F.B.; Funding acquisition, P.V.L., E.C.F. and L.B.P.; Investigation, P.V.L., R.P. and F.B.; Methodology, P.V.L. and R.P.; Project administration, E.C.F. and L.B.P.; Software, P.V.L.; Supervision, P.V.L., E.C.F. and L.B.P.; Validation, P.V.L. and F.B.; Visualization, P.V.L., R.P., F.B. and G.T.; Writing—original draft, R.P., P.V.L. and F.B.; Writing—review and editing, R.P., E.C.F. and P.V.L. All authors have read and agreed to the published version of the manuscript.

Funding: This research was funded by Norte Energia, via R&D Project registered with the PD-07427-0318/2018 code in ANEEL (Agência Nacional de Energia Elétrica) brokered by INESC P&D Brasil. It was also funded by CNPq (Conselho Nacional de Desenvolvimento Científico e Tecnológico), grant number 142331/2019-8.

Institutional Review Board Statement: Not applicable.

Informed Consent Statement: Not applicable.

Data Availability Statement: Not applicable.

Conflicts of Interest: The authors declare no conflict of interest. The funders had no role in the design of the study; in the collection, analyses, or interpretation of data; in the writing of the manuscript, or in the decision to publish the results.

References

- Pereira, M.V.F.; Pinto, L.M.V.G. Stochastic optimization of a multireservoir hydroelectric system: A decomposition approach. *Water Resour. Res.* **1985**, *21*, 779–792. [\[CrossRef\]](#)
- De Queiroz, A.R. Stochastic hydro-thermal scheduling optimization: An overview. *Renew. Sustain. Energy Rev.* **2016**, *62*, 382–395. [\[CrossRef\]](#)
- Pedrini, R.; Finardi, E.C. Long-term generation scheduling: A tutorial on the practical aspects of the problem solution. *J. Control Autom. Electr. Syst.* **2022**. [\[CrossRef\]](#)
- Finardi, E.C.; Decker, B.U.; de Matos, V.L. An introductory tutorial on stochastic programming using a long-term hydrothermal scheduling problem. *J. Control Autom. Electr. Syst.* **2013**, *24*, 361–376. [\[CrossRef\]](#)
- Noakes, D.J.; McLeod, A.I.; Hipel, K.W. Forecasting monthly riverflow time series. *Int. J. Forecast.* **1985**, *1*, 179–190. [\[CrossRef\]](#)
- Infanger, G.; Morton, D.P. Cut sharing for multistage stochastic linear programs with interstage dependency. *Math. Program.* **1996**, *75*, 241–256. [\[CrossRef\]](#)
- Maceira, M.E.P.; Duarte, V.S.; Penna, D.D.J.; Moraes, L.A.M.; Melo, A.C.G. Ten years of application of stochastic dual dynamic programming in official and agent studies in Brazil—Description of the NEWAVE program. In Proceedings of the 16th PSCC, Glasgow, Scotland, 14–18 July 2008; Volume 7, pp. 14–18.
- Tilmant, A.; Pinte, D.; Goor, Q. Assessing marginal water values in multipurpose multireservoir systems via stochastic programming. *Water Resour. Res.* **2008**, *44*. [\[CrossRef\]](#)
- Goor, Q.; Kelman, R.; Tilmant, A. Optimal multipurpose-multireservoir operation model with variable productivity of hydropower plants. *J. Water Resour. Plan. Manag.* **2011**, *137*, 258–267. [\[CrossRef\]](#)
- Gjerden, K.S.; Helseth, A.; Mo, B.; Warland, G. Hydrothermal scheduling in Norway using stochastic dual dynamic programming; A large-scale case study. In Proceedings of the 2015 IEEE Eindhoven PowerTech, Eindhoven, The Netherlands, 29 June–2 July 2015; pp. 1–6.
- Maceira, M.E.P.; Damazio, J.M. The use of PAR(p) model in the stochastic dual dynamic programming optimization scheme used in the operation planning of the Brazilian hydropower system. In Proceedings of the 2004 International Conference on Probabilistic Methods Applied to Power Systems, Ames, IA, USA, 12–16 September 2004; pp. 397–402.
- De Matos, V.L.; Larroyd, P.V.; Finardi, E.C. Assessment of the long-term hydrothermal scheduling operation policies with alternative inflow modeling. In Proceedings of the 2014 Power Systems Computation Conference IEEE, Wrocław, Poland, 18–22 August 2014; pp. 1–7.
- Hjelmeland, M.N.; Helseth, A.; Korpås, M. Medium-term hydropower scheduling with variable head under inflow, energy and reserve capacity price uncertainty. *Energies* **2019**, *12*, 189. [\[CrossRef\]](#)
- Yildiran, U. Nonnegative wind speed time series models for SDDP and stochastic programming applications. In Proceedings of the 2019 IEEE PES Innovative Smart Grid Technologies Europe (ISGT-Europe), IEEE, Bucharest, Romania, 29 September–2 October 2019; pp. 1–5.
- Gjelsvik, A.; Mo, B.; Haugstad, A. Long- and medium-term operations planning and stochastic modelling in hydro-dominated power systems based on stochastic dual dynamic programming. In *Handbook of Power Systems I*; Pardalos, P.M., Rebennack, S., Pereira, M.V.F., Iliadis, N.A., Eds.; Energy Systems; Springer: Berlin/Heidelberg, Germany, 2010; pp. 33–55. ISBN 978-3-642-02492-4.

16. Lima, L.M.M.; Popova, E.; Damien, P. Modeling and forecasting of Brazilian reservoir inflows via dynamic linear models. *Int. J. Forecast.* **2014**, *30*, 464–476. [[CrossRef](#)]
17. Shapiro, A.; Tekaya, W.; da Costa, J.P.; Soares, M.P. Risk neutral and risk averse stochastic dual dynamic programming method. *Eur. J. Oper. Res.* **2013**, *224*, 375–391. [[CrossRef](#)]
18. De Matos, V.L.; Finardi, E.C. A computational study of a stochastic optimization model for long term hydrothermal scheduling. *Int. J. Electr. Power Energy Syst.* **2012**, *43*, 1443–1452. [[CrossRef](#)]
19. Pritchard, G. Stochastic inflow modeling for hydropower scheduling problems. *Eur. J. Oper. Res.* **2015**, *246*, 496–504. [[CrossRef](#)]
20. Treistman, F.; Maceira, M.E.P.; Damázio, J.M.; Cruz, C.B. Periodic time series model with annual component applied to operation planning of hydrothermal systems. In Proceedings of the 2020 International Conference on Probabilistic Methods Applied to Power Systems (PMAAPS), Liege, Belgium, 18–21 August 2020; pp. 1–6.
21. Beltrán, F.; Finardi, E.C.; Fredo, G.M.; de Oliveira, W. Improving the performance of the stochastic dual dynamic programming algorithm using chebyshev centers. *Optim. Eng.* **2020**. [[CrossRef](#)]
22. De Matos, V.L.; Philpott, A.B.; Finardi, E.C. Improving the performance of stochastic dual dynamic programming. *J. Comput. Appl. Math.* **2015**, *290*, 196–208. [[CrossRef](#)]